PROCEEDINGS OF SCIENCE

Recent results from SND detector at VEPP-2000 collider

Achasov M.N.[ab], **Barnyakov A.Yu.**[ac], **Baykov A.A.**[ab], **Beloborodov K.I.**[ab], **Berdyugin A.V.***[ab], **Bogdanchikov A.G.**[a], **Botov A.A.**[a], **Dimova T.V.**[ab], **Druzhinin V.P.**[ab], **Golubev V.B.**[a], **Kardapoltsev L.V.**[ab], **Kharlamov A.G.**[ab], **Korol A.A.**[ab], **Kovrizhin D.P.**[a], **Kupich A.S.**[ab], **Martin K.A.**[a], **Melnikova N.A.**[a], **Muchnoy N.Yu.**[ab], **Obrazovsky A.E.**[a], **Pakhtusova E.V.**[a], **Pugachev K.V.**[ab], **Savchenko Ya.S.**[ab], **Serednyakov S.I.**[ab], **Shtol D.A.**[a], **Silagadze Z.K.**[ab], **Surin I.K.**[a], **Usov Yu.V.**[a], **Zhabin V.N.**[ab] **and Zhulanov V.V.**[ab].

[a] *Budker Institute of Nuclear Physics, Novosibirsk, 630090, Russia*
[b] *Novosibirsk State University, Novosibirsk, 630090, Russia*
[c] *Novosibirsk State Tecnical University, Novosibirsk, 630092, Russia*
E-mail: berdugin@inp.nsk.su

Recent results on e^+e^- annihilation to hadrons obtained in the SND experiment at the VEPP-2000 collider are presented. The data collected in 2010-2018 in the energy region below 2 GeV are analyzed. The processes $e^+e^- \to \pi^+\pi^-$, $n\bar{n}$, $\eta\pi^0\gamma$, $\pi^+\pi^-\pi^0$ are studied. Search for e^+e^- annihilation to C-even resonance $f_1(1285)$ is performed.

40th International Conference on High Energy physics - ICHEP2020
July 28 - August 6, 2020
Prague, Czech Republic (virtual meeting)

*Speaker.

PoS(ICHEP2020)452

1. Introduction

SND is a general-purpose non-magnetic detector [1, 2, 3, 4] collecting data at the VEPP-2000 e^+e^- collider [5]. Its main part is a three-layer spherical electromagnetic calorimeter consisting of 1630 NaI(Tl) crystals. The calorimeter energy and angular resolutions depend on the photon energy E as $\sigma_E/E(\%) = 4.2\%/\sqrt[4]{E(\mathrm{GeV})}$ and $\sigma_{\phi,\theta} = 0.82^\circ/\sqrt{E(\mathrm{GeV})} \oplus 0.63^\circ$. Its total solid angle is 95% of 4π. Directions of charged particles are measured using a nine-layer drift chamber and one-layer proportional chamber in a common gas volume. The solid angle of the tracking system is 94% of 4π. Its angular resolution is 0.45° and 0.8° for the azimuthal and polar angles, respectively. A system of threshold aerogel Cherenkov counters located between the tracking system and the calorimeter is used for charged kaon identification. Outside the calorimeter, a muon detector consisting of proportional tubes and scintillation counters is placed.

The VEPP-2000 collider beam energy is determined using a beam-energy-measurement system based on the Compton back-scattering of laser photons on the electron beam. The accuracy of the beam-energy measurement is about 30 keV [6].

Simulation of the signal and the background processes takes into account radiative corrections [7]. The angular distribution of hard photon emitted from the initial state is generated according to Ref. [8]. Interactions of the particles produced in e^+e^- annihilation with the detector materials are simulated using the GEANT4 software [9]. The simulation takes into account variation of experimental conditions during data taking, in particular dead detector channels and beam-induced background. To take into account the effect of superimposing the beam background on the e^+e^- annihilation events, simulation uses special background events recorded during data taking with a random trigger. These events are superimposed on simulated events, leading to the appearance of additional tracks and photons in events.

Main physics task of SND is study of all possible processes of e^+e^- annihilation into hadrons below 2 GeV. This implies the measurement of the total hadronic cross section, which is calculated as the sum of exclusive cross sections, We also study of hadronization (dynamics of exclusive processes) and properties of vector mesons of the ρ, ω, ϕ families. Currently, about 15 hadronic processes are being analyzed.

In 2010–2013, data with an integrated luminosity of about 70 pb^{-1} were collected in the energy range 0.3–2.0 GeV. Then, during 2013–2016, the complex was modernized to work with electrons and positrons from the VEPP-5 injection complex. The second data sample with an integrated luminosity of about 250 pb^{-1} was collected from 2017 to the present. Currently, the accumulated integrated luminosity below (0.30–0.97 GeV), near (0.98–1.05 GeV), and above ϕ-meson resonance is 77, 31, and 209 pb^{-1}, respectively.

2. $e^+e^- \to \pi^+\pi^-$

The measurements of hadronic cross sections below 2 GeV are largely motivated by the need for high-precision calculation of the hadronic contribution to the muon anomalous magnetic moment. In particular, the $e^+e^- \to \pi^+\pi^-$ cross section in the energy region below 1 GeV gives the dominant contribution to this value and should be measured with an accuracy better than 1%.

Parameter	This work	SND at VEPP-2M
m_ρ, MeV	$775.3 \pm 0.5 \pm 0.6$	$774.6 \pm 0.4 \pm 0.5$
Γ_ρ, MeV	$145.6 \pm 0.6 \pm 0.8$	$146.1 \pm 0.8 \pm 1.5$
$B_{\rho\to e^+e^-} \times B_{\rho\to\pi^+\pi^-}$	$(4.889 \pm 0.015 \pm 0.039) \times 10^{-5}$	$(4.876 \pm 0.023 \pm 0.064) \times 10^{-5}$
$B_{\omega\to e^+e^-} \times B_{\omega\to\pi^+\pi^-}$	$(1.318 \pm 0.051 \pm 0.021) \times 10^{-6}$	$(1.225 \pm 0.058 \pm 0.041) \times 10^{-6}$

Table 1: Results of the fit to the $e^+e^- \to \pi^+\pi^-$ cross section obtained in this work in comparison with the results of SND at VEPP-2M [11] The first error is statistical, the second is systematic.

In this report, we present the results of the $e^+e^- \to \pi^+\pi^-$ cross section measurement in the energy region $525 \le \sqrt{s} \le 883$ MeV based on the 4.6 pb$^-$1 data sample recorded by SND in 2012–2013 [10]. Approximately 2.3×10^6 collinear two-body events are selected. From them about 10^6 events are from the processes $e^+e^- \to \pi^+\pi^-$ and $e^+e^- \to \mu^+\mu^-$, and 1.3×10^6 are from the $e^+e^- \to e^+e^-$. The obtained $e^+e^- \to \pi^+\pi^-$ cross section is shown in Fig. 1). The systematic uncertainty of the cross section measurement is 0.8% at $\sqrt{s} > 600$ MeV. In the framework of the vector meson dominance (VMD) model the $e^+e^- \to \pi^+\pi^-$ cross section in energy region under study is described by a sum of contributions of the vector meson resonances ρ, ω, and ρ'. The result of the fit with this model is shown in Fig. 1). The obtained ρ-meson parameters and the product $B_{\omega\to e^+e^-}B_{\omega\to\pi^+\pi^-}$ are listed in Table 1) in comparison with the results of the previous SND measurement performed at the VEPP-2M collider [11].

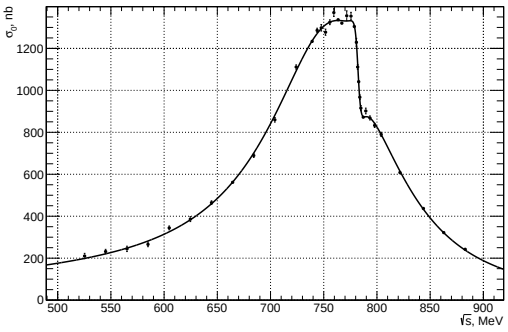

Figure 1: The $e^+e^- \to \pi^+\pi^-$ cross section measured by SND (points with error bars). The curve is the result of the VMD fit.

Using the obtained cross section data we calculate the contribution from the $e^+e^- \to \pi^+\pi^-$ channel in the energy region $525 \le \sqrt{s} \le 883$ MeV to the muon anomalous magnetic moment $a_\mu(\pi\pi)$. Our result is compared with the $a_\mu(\pi\pi)$ values calculated using the cross section data obtained by SND@VEPP-2M [11], BABAR [12], and KLOE [13]. The differences between this work, SND@VEPP-2M and BABAR do not exceed one standard deviation. The difference with KLOE is 1.3σ.

3. $e^+e^- \to \pi^+\pi^-\pi^0$

The process $e^+e^- \to \pi^+\pi^-\pi^0$ was studied in many experiments. Currently the $e^+e^- \to$

Measurement	$a_\mu(\pi\pi)\times 10^{10}$
This work	$409.79 \pm 1.44 \pm 3.87$
SND at VEPP-2M	$406.47 \pm 1.74 \pm 5.28$
BaBar	$413.58 \pm 2.04 \pm 2.29$
KLOE	$403.39 \pm 0.72 \pm 2.50$

Table 2: The contribution to the anomalous magnetic moment of the muon $a_\mu(\pi\pi$, 525 MeV $\leq \sqrt{s} \leq$ 883 MeV) $\times 10^{10}$ calculated using cross section data from different experiments.

$\pi^+\pi^-\pi^0$ cross section is measured in detail in the center-of-mass (c.m.) energy ($\sqrt{s}$) range from 0.6 GeV to 3 GeV. The most accurate data were obtained in the SND [14], CMD-2 [15] and BABAR [16] experiments. It is usually assumed that the dominant intermediate mechanism of this process is $\rho\pi$. In the energy region 1–2 GeV there is a small contribution of the $\omega\pi$ intermediate state. In Ref. [16] a significant deviation from the $\rho\pi$ model is observed in the two-pion invariant mass spectra, which may be explained by the contribution of the $\rho(1450)\pi$ intermediate state.

In this work [17], we measure $e^+e^- \to \pi^+\pi^-\pi^0$ cross section and study the dynamics of this process in the region $\sqrt{s} = 1.1$–2.0 GeV. The cross section is measured with a systematic uncertainty of 4.4%. The result of the fit to the measured cross section with the VMD model is shown in Fig. 2). The two peaks in the cross section corresponds to the $\omega(1420)$ and $\omega(1650)$ resonances.

To study the dynamics of the process $e^+e^- \to \pi^+\pi^-\pi^0$, we analyze the Dalitz plot distribution and the spectrum of the $\pi^+\pi^-$ invariant mass. The data distributions are fitted with the model including the $\rho(770)\pi$, $\rho(1450)\pi$, and $\omega\pi^0$ intermediate states. The modulus squared of the $\omega\pi^0$ amplitude has been fixed from our measurement of the $e^+e^- \to \omega\pi^0 \to \pi^0\pi^0\gamma$ cross section [18]. As a result of the fit, the cross sections $\sigma_{\rho\pi}$ and $\sigma_{\rho'\pi}$, which are proportional to the modulus squared of $\rho(770)\pi$ and $\rho(1450)\pi$ amplitudes, respectively, and the relative phases between the $\rho(770)\pi$ amplitude and the $\rho(1450)\pi$ and $\omega\pi^0$ amplitudes are obtained for 14 energy intervals. In Fig. 2) we show the obtained $\sigma_{\rho\pi}$, $\sigma_{\rho'\pi}$, and $\sigma_{\omega\pi^0}$ values in comparison with the total $e^+e^- \to \pi^+\pi^-\pi^0$ cross section. The cross section for the intermediate state $\rho(1450)\pi$ differs significantly from zero in the range 1.55–1.75 GeV, where the resonance $\omega(1650)$ is located. In the $\rho(770)\pi$ cross section the resonance structure near 1650 MeV is not observed. We conclude that the intermediate state $\rho(1450)\pi$ gives a significant contribution to the decay $\omega(1650) \to \pi^+\pi^-\pi^0$, and that the $\omega(1420) \to \pi^+\pi^-\pi^0$ decay is dominated by the $\rho(770)\pi$ intermediate state.

4. $e^+e^- \to \eta\pi^0\gamma$

The dominant contribution to the $e^+e^- \to \eta\pi^0\gamma$ cross section in the energy region 1.05–2 GeV is expected to come from the process $e^+e^- \to \omega\eta$ with the decay $\omega \to \pi^0\gamma$. This process was measured in the BABAR, CMD-3 and SND experiments in the decay mode $\omega \to \pi^+\pi^-\pi^0$. These measurement were performed neglecting the interference between the $\omega\eta$ and other intermediate mechanisms ($a_0(980)$, $\rho(1450)\pi$ and $\phi\eta$) contributing to the $e^+e^- \to \pi^+\pi^-\pi^0\eta$ reaction. The

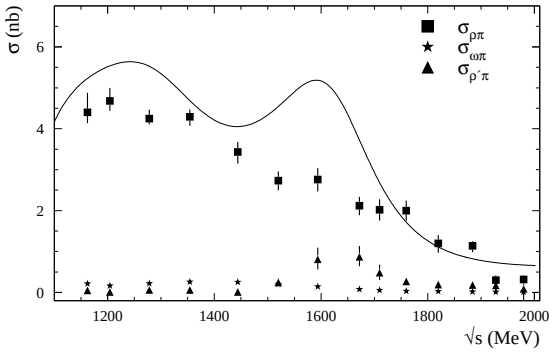

Figure 2: The measured energy dependences of the cross sections $\sigma_{\rho\pi}$, $\sigma_{\rho'\pi}$, and $\sigma_{\omega\pi}$, The curve is the result of the fit to the SND data on the total $e^+e^- \to \pi^+\pi^-\pi^0$ cross section.

measurements obtained under this assumption need additional verification, especially in the region $\sqrt{s}$ = 1.85–2.00 GeV, where the $e^+e^- \to \omega\eta$ cross section is almost zero (less 50 pb) compared to the significant ($\sim$ 2 nb) contribution from other mechanisms.

The most interesting in the $e^+e^- \to \eta\pi^0\gamma$ reaction is the contribution of radiative decays of excited vector mesons of the ρ, ω and ϕ families to $a_0(980)\gamma$, $a_2(1320)\gamma$, and $a_0(1450)\gamma$. The measurement of these decays is important for understanding the quark structure of excited vector mesons. In particular, there are indications that the excited states of the ρ and ω mesons may contain an admixture of a vector hybrid state. The widths of the radiation decays are sensitive to the hybrid admixture.

In this report we present the study of the process $e^+e^- \to \eta\pi^0\gamma$ in the center-of-mass energy range 1.05 – 2.00 GeV using data with an integrated luminosity of 94.5 pb^{-1} [19]. The $e^+e^- \to \eta\pi^0\gamma$ cross section in this energy region is measured for the first time. The main contribution to the cross section arises from the intermediate mechanism $\omega\eta$. The measured cross section for the subprocess $e^+e^- \to \omega\eta \to \eta\pi^0\gamma$ agrees well with the previous measurements by SND and CMD-3 in the decay mode $\omega \to \pi^+\pi^-\pi^0$. The significantly smaller contribution to the $e^+e^- \to \eta\pi^0\gamma$ cross section from other hadronic intermediate states $\rho\eta$, $\phi\eta$, $\phi\pi^0$, $\omega\pi^0$, and $\rho\pi^0$ is calculated using existing data on their production cross section. It is found, with a significance of 5.6σ, that the process $e^+e^- \to \eta\pi^0\gamma$ is not completely described by the hadronic intermediate states. We assume that the missing contribution (rad-$\eta\pi\gamma$) arises from radiative processes, e.g. $e^+e^- \to a_0(980)\gamma$, $a_0(1450)\gamma$, and $a_2(1320)\gamma$. The measured cross section for the process $e^+e^- \to rad - \eta\pi^0\gamma$ is shown in Fig. 3. It is 15–20 pb in a wide energy range, from 1.3 to 1.9 GeV. The spectrum of $\eta\pi^0$ invariant masses for the events rad-$\eta\pi^0\gamma$ is consistent with the dominance of the intermediate mechanism $a_0(1450)\gamma$.

5. $e^+e^- \to f_1(1285)$

The dominant mechanism of hadron production in e^+e^- collisions is single-photon annihilation. Annihilation through two photons is suppressed by a factor of α^2, where α is the fine structure constant. The only observed process of the two-photon annihilation into hadrons in e^+e^- collisions

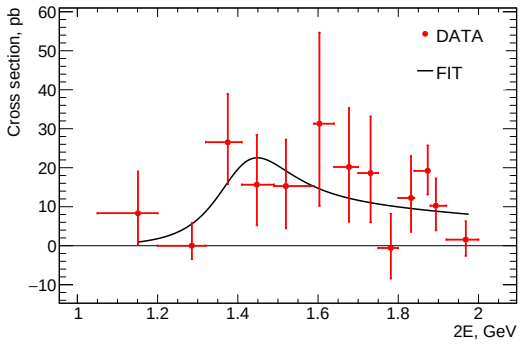

Figure 3: The measured cross section for the process $e^+e^- \to rad - \eta\pi^0\gamma$ (points with error bars). The curve is the result of the VMD fit.

$\sqrt{s}$ (GeV)	L (nb^{-1})	N	N_{bkg}	$\sqrt{s}$ (GeV)	L (nb^{-1})	N	N_{bkg}
1.200	1185	0	0.054 ± 0.010	1.300	2220	0	0.108 ± 0.021
1.225	577	0	0.028 ± 0.005	1.325	559	0	0.037 ± 0.007
1.250	467	0	0.025 ± 0.005	1.350	1945	0	0.124 ± 0.022
1.275	516	0	0.022 ± 0.005	1.360	826	0	0.080 ± 0.012
1.280	740	0	0.045 ± 0.008	1.375	612	0	0.057 ± 0.008
1.282	3451	2	0.252 ± 0.044	1.400	2024	0	0.275 ± 0.032

Table 3: The center-of-mass energy ($\sqrt{s}$), integrated luminosity (L), number of selected data events (N), number of background events (N_{bkg}) calculated using simulation with the statistical error.

is the production of two vector mesons, $\rho^0\rho^0$ and $\rho^0\phi$, in the BABAR experiment [20]. Experiments on the search for production of a single C-even resonance began more than 30 years ago at the VEPP-2M e^+e^- collider with the ND detector [21]. In these experiments, the first upper limits were set on the probabilities of the inverse reactions, namely the decays η', $f_0(975)$, $f_2(1270)$, $f_0(1300)$, $a_0(980)$, and $a_2(1320)$ to e^+e^- pairs. In recent experiments at the colliders VEPP-2M, VEPP-2000 and BEPCII, this inverse-reaction technique was used to set the best upper limits on the electron widths of the resonances listed above, as well as η and $X(3872)$.

We analyze [22] data with an integral luminosity of 15.1 pb^{-1}, recorded in 2010–2012 and 2017 in the center-of-mass energy region $\sqrt{s} = 1.2$–1.4 GeV at 12 energy points listed in Table 3. The data set at the maximum of the f_1 resonance $\sqrt{s}$ = 1.282 GeV with an integral luminosity of 3.45 pb^{-1} was collected in 2017 specially for this analysis. For 2010–2012 energy scans the collider energy was controlled with an accuracy of 2–4 MeV. In 2017 the beam energy was monitored with an accuracy of about 80 keV by the backscattering-laser-light system. The center-of-mass energy spread at $\sqrt{s} = 1.282$ GeV is 630 keV.

The search for the process $e^+e^- \to f_1(1285)$ is performed in the decay channel $f_1(1285) \to \eta\pi^0\pi^0$ with the subsequent decays $\eta \to \gamma\gamma$ and $\pi^0 \to \gamma\gamma$. Since the final state for the process under study does not contain charged particles, the process without charged particles $e^+e^- \to \gamma\gamma$ is used for normalization. After applying the selection criteria, two events have been observed at the peak of the $f_1(1285)$ resonance and zero events beyond the resonance (see Table 3). These two events

correspond to the cross section $\sigma(e^+e^- \to f_1) = 45^{+33}_{-24}$ pb and the branching fraction $B(f_1(1285) \to e^+e^-) = (5.1^{+3.7}_{-2.7}) \times 10^{-9}$. The significance of the $e^+e^- \to f_1(1285)$ signal is 2.5σ. We consider this result as a first indication of the process $e^+e^- \to f_1(1285)$. The measured branching fraction agrees with the theoretical predictions [23, 24].

6. $e^+e^- \to n\bar{n}$

We present the preliminary results of the $e^+e^- \to n\bar{n}$ measurement based on the 2017 dataset. The method used in this analysis differs from that used in the previous SND analysis [25]. We analyze the distribution of the event time measured in the calorimeter with respect to the beam collision time shown in Fig. 4. The number of signal events is determined from the fit to this distribution with a sum of signal, cosmic background, and beam-induced background time spectra.

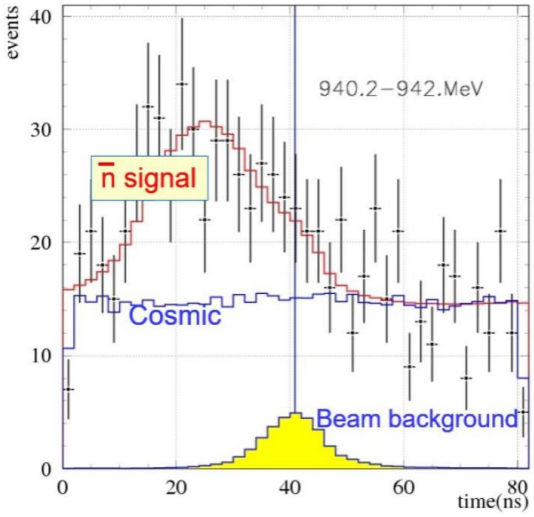

Figure 4: The event time distribution for selected $e^+e^- \to n\bar{n}$ candidate events (points with error bars) fitted by a sum of distributions for signal, cosmic background, and beam background.

The preliminary result on the $e^+e^- \to n\bar{n}$ cross section is shown in Fig. 5 in comparison with the previous measurements. The new measurements is lower than the previous SND measurement [25]. The reasons are underestimated beam background and incorrect MC simulation. The systematic uncertainty on the cross section is estimated to be about 20%, mainly due to data-MC simulation difference in detector response for antineutron.

The $e^+e^- \to n\bar{n}$ cross section is given by the following expression:

$$\frac{d\sigma}{d\Omega}(s,\theta) = \frac{\alpha^2\beta}{4s}\left[|G_M(s)|^2(1+cos^2\theta) + \frac{1}{\tau}|G_E(s)|^2 sin^2\theta\right], \tag{6.1}$$

where α is the fine structure constant, $\beta = \sqrt{1-4m_n^2/s}$, m_n is neutron mass, $\tau = \sqrt{(s)}/(2m_n)$, θ is the antineutron polar angle, and G_E and G_M are neutron electric and magnetic form factors, respectively. We study the antineutron angular distribution shown in Fig. 6 and obtain the ratio of the form factors $|G_E|/|G_M| = 1.35 \pm 0.35$.

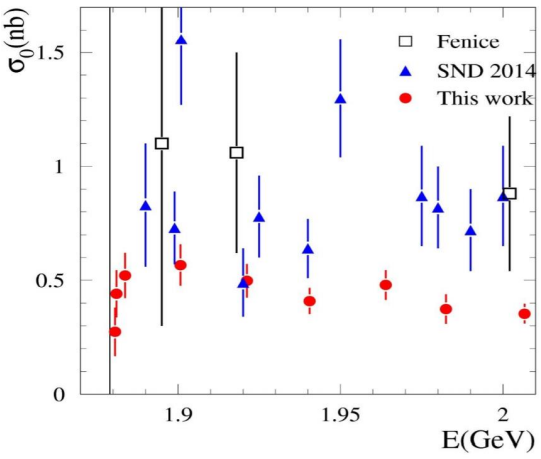

Figure 5: The $e^+e^- \to n\bar{n}$ cross section measured in this work (preliminary result) in comparison with previous measurements.

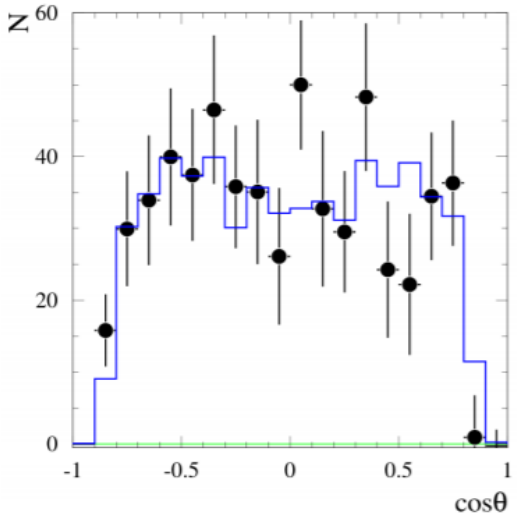

Figure 6: The cos θ distribution for $e^+e^- \to n\bar{n}$ data events (points with error bars). The histogram is the result of the fit with a sum of simulated distributions for the G_E and G_M terms in Eq. 6.1.

References

[1] M. N. Achasov *et al.*, Nucl. Instrum. Meth. A **598**, 31 (2009).

[2] V. M. Aulchenko *et al.,* A **598**, 102 (2009).

[3] A. Yu. Barnyakov *et al.,* A **598**, 163 (2009).

[4] V. M. Aulchenko *et al.,* A **598**, 340 (2009).

[5] P. Y. Shatunov *et al.*, Phys. Part. Nucl. Lett. **13**, no. 7, 995 (2016).

[6] E.V. Abakumova *et al.*, Nucl. Instr. Meth.A **744** (2014) 35-40 [arXiv:1310.7764]

[7] E. A. Kuraev and V. S. Fadin, Sov. J. Nucl. Phys. **41**, 466 (1985) [Yad. Fiz. **41**, 733 (1985)].

[8] G. Bonneau and F. Martin, Nucl. Phys. B **27**, 381 (1971).

[9] S. Agostinelli *et al.* [GEANT4 Collaboration], Nucl. In- strum. Meth. A **506**, 250 (2003).

[10] M. N. Achasov *et al.* (SND Collaboration), arXiv:2004.00263.

[11] M.N. Achasov *et al.* (SND Collaboration), J.Exp.Theor.Phys. **103**, 380 (2006) [arXiv:hep-ex/0605013].

[12] B. Aubert *et al.* (BABAR Collaboration), Phys. Rev. Lett. **103**, 231801 (2009).

[13] A. Anastasi *et al.* (KLOE Collaboration), JHEP **1803**, 173 (2018) [arXiv:1711.03085].

[14] M. N. Achasov *et al.* (SND Collaboration), Phys. Rev. D **63**, 072002 (2001); Phys. Rev. D **66**, 032001 (2002); Phys. Rev. D **68**, 052006 (2003).

[15] R. R. Akhmetshin *et al.* (CMD-2 Collaboration), Phys. Lett. B **578**, 285 (2004); Phys. Lett. B **642**, 203 (2006).

[16] B. Aubert *et al.* (BABAR Collaboration), Phys. Rev. D **70**, 072004 (2004).

[17] M. N. Achasov *et al.* (SND Collaboration), arXiv:2007.14595.

[18] M. N. Achasov *et al.* (SND Collaboration), Phys. Rev. D **94**, 112001 (2016).

[19] M. N. Achasov *et al.* (SND Collaboration), arXiv:2006.05465.

[20] B. Aubert *et al.* (BABAR Collaboration), Phys. Rev. Lett. **97**, 112002 (2006) [hep-ex/0606054].

[21] P. V. VorobâĂŹev *et al.* (ND Collaboration), Sov. J. Nucl. Phys. 48, 273 (1988) [Yad. Fiz. 48, 436 (1988)].

[22] M. N. Achasov *et al.* (SND Collaboration), Phys. Lett. B **800**, 135074 (2020) [arXiv:1906.03838].

[23] A. S. Rudenko, Phys. Rev. D **96**, 076004 (2017) [arXiv:1707.00545].

[24] A. I. Milstein and A. S. Rudenko, Phys. Lett. B **800**, 135117 (2020) [arXiv:1909.07938].

[25] M.N. Achasov *et.al.* (SND Collaboration), Phys. Rev. D **90**, 112007 (2014).